

## Towards a magnetoresistive platform for neural signal recording

P. P. Sharma, G. Gervasoni, E. Albisetti, F. D'Ercoli, M. Monticelli, D. Moretti, N. Forte, A. Rocchi, G. Ferrari, P. Baldelli, M. Sampietro, F. Benfenati, R. Bertacco, and D. Petti

Citation: *AIP Advances* **7**, 056706 (2017); doi: 10.1063/1.4973947

View online: <http://dx.doi.org/10.1063/1.4973947>

View Table of Contents: <http://aip.scitation.org/toc/adv/7/5>

Published by the *American Institute of Physics*

---

---

## Towards a magnetoresistive platform for neural signal recording

P. P. Sharma,<sup>1</sup> G. Gervasoni,<sup>2</sup> E. Albisetti,<sup>1</sup> F. D'Ercoli,<sup>1</sup> M. Monticelli,<sup>1</sup> D. Moretti,<sup>3</sup> N. Forte,<sup>3</sup> A. Rocchi,<sup>3</sup> G. Ferrari,<sup>2</sup> P. Baldelli,<sup>3</sup> M. Sampietro,<sup>2</sup> F. Benfenati,<sup>3</sup> R. Bertacco,<sup>1</sup> and D. Petti<sup>1</sup>

<sup>1</sup>*Department of Physics, Politecnico di Milano, Milan 20133, Italy*

<sup>2</sup>*Department of Electronics, Information and Bioengineering, Politecnico di Milano, Milan 20133, Italy*

<sup>3</sup>*Center of Synaptic Neuroscience, Italian Institute of Technology, Genova 16132, Italy*

(Presented 1 November 2016; received 23 September 2016; accepted 24 October 2016; published online 10 January 2017)

A promising strategy to get deeper insight on brain functionalities relies on the investigation of neural activities at the cellular and sub-cellular level. In this framework, methods for recording neuron electrical activity have gained interest over the years. Main technological challenges are associated to finding highly sensitive detection schemes, providing considerable spatial and temporal resolution. Moreover, the possibility to perform non-invasive assays would constitute a noteworthy benefit. In this work, we present a magnetoresistive platform for the detection of the action potential propagation in neural cells. Such platform allows, in perspective, the in vitro recording of neural signals arising from single neurons, neural networks and brain slices. © 2017 Author(s). All article content, except where otherwise noted, is licensed under a Creative Commons Attribution (CC BY) license (<http://creativecommons.org/licenses/by/4.0/>). [<http://dx.doi.org/10.1063/1.4973947>]

### INTRODUCTION

Understanding brain functions through the investigation of neural signals from single neurons or neural arrays is a key aspect for further studies on neurologic disease and related therapies. In order to address the latter topic, many technological solutions have been proposed. Currently, the most widespread neural signal detection scheme relies on an electrophysiological approach through the patch clamp technology or the local field potential recording (LFP).<sup>1</sup> The former technique consists in stimulating the cells and recording the real-time voltage drop across the cell membrane that occurs because of the ionic channels opening, while the latter enables recording the voltage perturbation generated in the extracellular space by neuronal activity, from fast action potential to the slowest voltage fluctuations arising from glia.<sup>2</sup> Such methods achieve a considerable sensitivity but fails to provide signals simultaneously from more than a couple of neurons.<sup>3</sup> The strong progress of micro-fabrication techniques has allowed for the development of alternative methods like multi electrode arrays (MEAs) and high density MEAs (hdMEAs) which consist of numerous electrode-containing plates and grant the recording at a network level.<sup>4-6</sup> However, such approach is inefficient in providing a one-to-one correlation between the investigated neurons and the acquired signals.<sup>7</sup> More recently, nano-scale electrodes and nano-sized field effect transistors have been successfully employed for neural signal recording.<sup>8-10</sup> Even though the spatial resolution was not significantly increased with respect to conventional MEAs and the signal to noise ratio resulted diminished when compared to standard glass pipettes, these techniques provided an extremely reduced invasiveness on the biological sample and presented potentiality for higher density packing.<sup>11</sup> High spatial resolution together with non-invasiveness has been obtained by investigating neural activity through calcium imaging by means of calcium indicators GCaMP.<sup>12,13</sup> A complete absence of invasiveness together with good spatial resolution can be also assured by using a magnetic approach. Instead of directly measuring the voltage across the cell membrane, one can detect the magnetic field generated by the neural current along the axon, arising from the charge displacement across the membrane. With this

approach, nanometer spatial resolution was obtained employing the promising technology based on diamond nitrogen vacancies (NV).<sup>14</sup> Nevertheless, current magnetometers based on NV still display poor temporal resolution.<sup>15</sup>

To tackle the aforementioned issues, magnetoresistive (MR) devices offer valuable perspectives because of their high sensitivities,<sup>16</sup> and easy real-time monitoring of the neural signals due to the wide frequency bandwidth.<sup>17,18</sup> Finally, as the detection does not involve any charge drain from neurons, they guarantee a complete absence of invasiveness during recording. Such technique has been firstly introduced by *J. Amaral et al.* who used spin valve featuring giant magnetoresistance (GMR) effect as magnetic sensors.<sup>19</sup> Sizable signals have been reported but in that work the presence of spurious capacitive signals was a big obstacle to a pure magnetic detection.

In this work, we present a platform based on different MR sensors, namely magnetic tunneling junctions (MTJs), and dedicated electronics for the detection of neural pulses generated by single neurons, neural networks and brain slice.

In the following, a brief description of the sensors fabrication process and main characteristics are presented. Studies on biocompatible capping solutions, ensuring good adhesion of neural cells and viability during at least two weeks, are discussed. Finally, the electronic measurement setup for the signal recording is illustrated.

## EXPERIMENTAL

### MTJ sensors fabrication

MTJs were fabricated on top of Si/SiO<sub>2</sub> wafers. The complete stack Ta(5)/ Ru(18)/ Ta(3)/ Ir<sub>20</sub>Mn<sub>80</sub>(20)/ CoFe(1.7)/ Ru (0.9)/ Co<sub>40</sub>Fe<sub>40</sub>B<sub>20</sub>(2.7)/ MgO (2.2)/ Co<sub>40</sub>Fe<sub>40</sub>B<sub>20</sub>(1.25)/ Ru(5)/ Ta(20), (thicknesses in nm within brackets), was deposited by magnetron sputtering in an AJA ORION 8 system and processed afterwards with optical lithography and ion milling.<sup>20</sup> A Ti(7)/Au(200) contact bilayer was deposited on top via magnetron sputtering with a Leybold Heraeus machine. The final chip layout (Fig.1 (a)) featured an array of 12 sensors with a junction area of 3x40 μm<sup>2</sup> (Fig. 2 (b)), each provided with independent access for electrical contact.<sup>21</sup> The sensors were subsequently annealed at 290°C for enabling the crystallization of the junction layers for promoting a coherent tunneling process.<sup>22,23</sup> The transfer curve of the sensors is shown in Fig.1(c); a magnetoresistive ratio of 44% was obtained together with a low field sensitivity of 10  $\frac{\%}{mT}$ . A linear response along with a negligible hysteresis was achieved by exploiting the superparamagnetic behavior of the free Co<sub>40</sub>Fe<sub>40</sub>B<sub>20</sub> layer and through the shape anisotropy enforced by the lithographic process.<sup>24</sup> These latter aspects, besides the low field sensitivity values, are fundamental conditions when small and repetitive signals are investigated.

### Neural culture on sensor surface and hippocampal brain slice preparation

In order to assure biocompatibility and to protect the sensors from the biological environment, a SiO<sub>2</sub>(50)/Si<sub>3</sub>N<sub>4</sub>(70)/SiO<sub>2</sub>(50) trilayer was deposited on top of the sensors by RF magnetron sputtering.

All experiments were carried out in accordance with the guideline as established by the European Community Council (Directive 2010/63/EU of September 22nd, 2010) and experimental protocols were approved by the Italian Ministry of Health. Animals were anaesthetized with isoflurane prior to decapitation.

Neurons were cultured over the sensors surface following standard protocols.<sup>25</sup> Prior to the growth of neural cells, an oxygen plasma treatment was performed on the chip for 1 min at 100 W. Subsequently, the chips were cleaned in ethanol (75%) for ten minutes and afterwards kept under UV for 1 hour. To promote cell adhesion, the chip surface was coated with Poly-D-lysine (1 mg/1 ml; Sigma; mw 70000-150000) in buffer borate solution and incubated overnight. Eventually, cortical neurons from dissociate rat brain embryos (E18) were plated on the sensor surface (10<sup>6</sup> cells/ml). The media was changed after seven days in vitro (DIV).

Concerning the preparation of the brain slices, all experiments were performed on C57BL/6J mice of either sex aged 3 weeks to 6 months (Charles River Laboratories International, Wilmington,

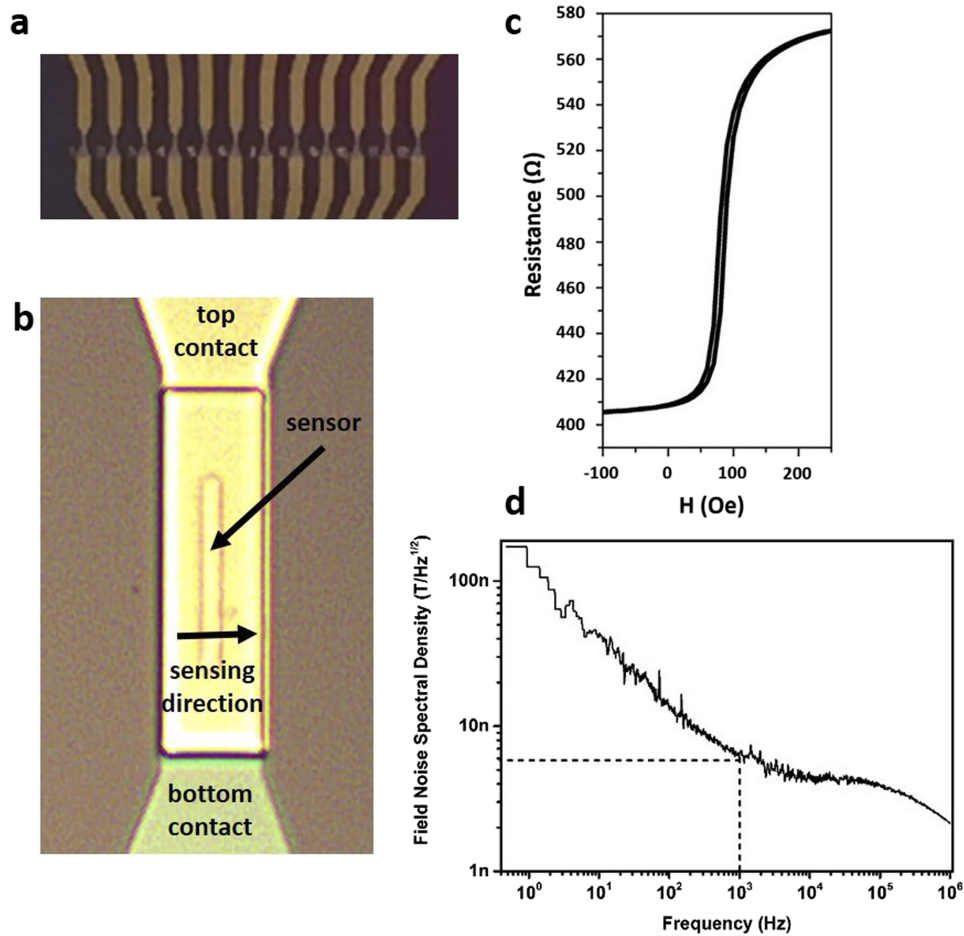


FIG. 1. (a) Sensors array comprising 12 MTJs, each with independent top and bottom contacts. (b) Optical image of the single sensor featuring a  $3 \times 40 \mu\text{m}^2$  area. (c) Transfer curve of the sensor, measured along the sensing direction. (d) Field noise spectral density measured at a bias field of 6 mT.

MA, USA). Transverse hippocampal slices (350  $\mu\text{m}$  thick) were cut using a Microm HM 650 V microtome equipped with a Microm CU65 cooling unit (Thermo Fisher Scientific, Waltham, MA). Slices were cut at  $\approx 2^\circ\text{C}$  in a high-sucrose protective solution containing (in mM): 87 NaCl, 25  $\text{NaHCO}_3$ , 2.5 KCl, 0.5  $\text{CaCl}_2$ , 7  $\text{MgCl}_2$ , 25 glucose, 75 sucrose, and saturated with 95%  $\text{O}_2$  and 5%  $\text{CO}_2$ . Slices were incubated for 30–45 min at  $35^\circ\text{C}$  and for at least another 30 min at room temperature in an artificial cerebrospinal fluid (ACSF) containing (in mM): 125 NaCl, 25  $\text{NaHCO}_3$ , 25 glucose, 2.5 KCl, 1.25  $\text{NaH}_2\text{PO}_4$ , 2  $\text{CaCl}_2$ , and 1  $\text{MgCl}_2$  (bubbled with 95%  $\text{O}_2$ –5%  $\text{CO}_2$ ). During the recording session the ACSF was perfused at a rate of 2.5 ml/min.<sup>26</sup>

### Magnetic platform and acquisition setup

A custom two faces PCB board, with a mass plane on one side and copper contact pads on the other, was designed in order to provide compatibility with LFP recording and allow the cellular growth rather than the insertion of the brain slices with the cerebrospinal fluids (Fig. 3(a)).

The PCB pads were aligned to the sensors pad and the attachment was realized by means of an anisotropic conductive tape (Adafruit 3M). The PCB board was holed in correspondence to the active area of the sensors and a culture chamber was sealed on top. The sealing was performed before the biological experiments, through PDMS, which was fabricated by mixing the elastomer and the curing agent in a 10:1 ratio and cured at  $60^\circ\text{C}$  for three hours. The PCB pads were connected to a dedicated electronic board.



The realized electronic board implements a generation channel and four low-noise acquisition channels working in parallel. The generation channel drives the magnetic sensors with a sinusoidal voltage signal of selectable amplitude (from few tens of  $\mu\text{V}$  up to 100 mV) and frequency (from few Hz up to 100 kHz). The front-end of each acquisition channel consists of a transimpedance amplifier with an input voltage noise of about  $3 \text{ nV}/\sqrt{\text{Hz}}$  (AD745 OpAmp from Analog Devices), followed by a Programmable Gain Amplifier, an anti-aliasing filter and an ADC operating at 833 kS/s. Exploiting the parallelism of a Field Programmable Gate Array (FPGA) the four acquired signals are simultaneously processed: phase/quadrature demodulation, selectable filtering and decimation. Finally, data are sent to the PC through a USB connection.

For the recording of the signals arising from the brain slice, the PCB device with the chip and the culture chamber were kept under an optical upright microscope, and two electrodes were used. A stimulating electrode was used to evoke action potential in the afferent fibers while a recording electrode was used for standard LFP measurements. Two permanent magnets were kept aside the chips in order to bias the sensors in their most sensitive points.

The measurements were performed by applying a 10 mV bias across the sensors at a frequency  $f = 40 \text{ kHz}$ , so as to get rid of the low-frequency noise of the electronic amplifier. The signal was then demodulated and filtered at  $4 \text{ kHz}$ , so as to allow for a sampling frequency four times faster than the maximum frequency in the bandwidth of the neural signal (about 1 kHz). The acquisition was operated with a sampling time of  $90 \mu\text{s}$ .

## RESULTS AND DISCUSSION

### Minimum detectable field

The field noise spectral density in Fig. 1 (d) was measured with a Correlation Spectrum Analyzer setup and the integrated spectrum was calculated.<sup>27</sup> Since the typical duration of the neural action potential is in the millisecond length, a kHz range was mainly taken into consideration. At 1 kHz, a noise spectral density for the whole sensing apparatus (including the sensor and the electronics) of about  $5 \text{ nT}/\sqrt{\text{Hz}}$  was found (Fig. 1 (d)), as measured within a 1 Hz narrow band. An integrated value of about 250 nT was calculated in a 1 Hz-1 kHz bandwidth, which is the typical bandwidth of neural signals. The reported values are comparable with or lower than the detectivities found in previous works.<sup>28,29</sup>

As a matter of fact, since the typical magnetic field, expected to be generated from a single neuron firing, ranges from 2 nT to 10 nT, only a narrow-band measurement would result in a successful detection. The latter configuration would also require a modulation of the magnetic field, and such feature is still under development.<sup>30,31</sup> On the other hand, a broad-band measurement configuration could be well utilized when an assembly of neurons are analyzed. The latter condition is verified when brain slices are considered, where several hundreds of cells potentially fire synchronously, resulting in much higher currents, and thus, magnetic field.

### Biocompatibility

A crucial aspect for ensuring an efficient growth of a neuronal culture on the sensor surface is to find a proper capping that enables cell viability and provides protection to the magnetic device. The presence of toxic materials as cobalt and manganese in the sensor stack represents the basic drawback for the cellular growth. Fig. 2 (a) shows an image of the cortical cultured neurons after two weeks in vitro. Fig 2(b) and (c) depict cell viability on the sensor and on a reference glass substrate, respectively.

A similar mortality rate, of almost 50%, (Fig. 2(d)), was obtained for cells plated on the sensor or on the reference substrate. The sensor was subsequently analyzed and no deterioration of its performance was found (data not shown).

### Recording from hippocampal brain slice

In this section, we present the platform for the recording of neural signal arising from rat hippocampal slices. These biological samples feature a dense assembly of fibers which, when electrically

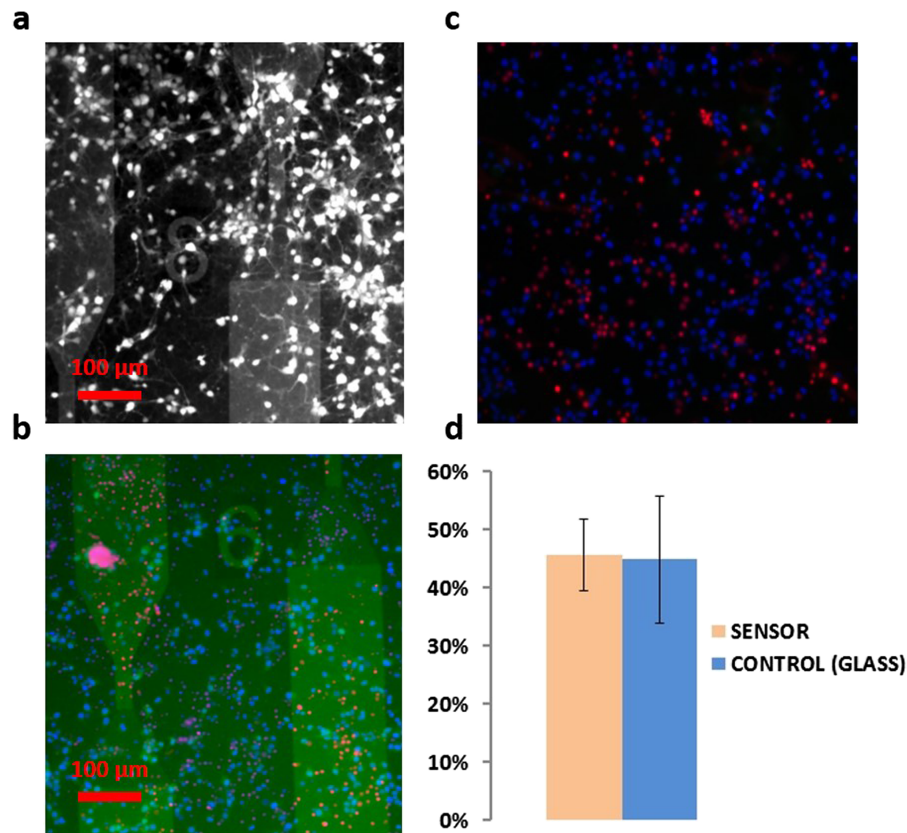


FIG. 2. (a) Transmitted light microphotograph of cortical neurons (14 DIV) plated on the sensor. (b) Fluorescent images of cortical neurons plated on the sensor and (c) on the reference glass substrate. Blue dots identify 4',6-diamidino-2-phenylindole (DAPI)-positive nuclei, while red dots represent dead cells that have internalized Propidium Iodure. (d) Bar histogram showing mean  $\pm$  sem of cellular viability of cortical neurons cultured for two weeks on the sensor (orange bar;  $n=1$ ) and on the reference slide (blue bar;  $n=1$ ).

stimulated, result in a potential activation of several hundred cell bodies. *J. Amaral et al.* evaluated such signal to be over  $2.5 \mu\text{T}$  at a  $10 \mu\text{m}$  distance.<sup>19</sup> This evaluation takes into account the presence of a layer of dead (inactive) cells arising from the slicing of the brain and the unavoidable distance between the sensor and the hippocampal slices. The brain slice is therefore an interesting tool in order to validate a MTJ-based platform for the neural activity recording.

The slice was positioned in such a way that the fibers were aligned to the long side of the sensors, so that the Oersted field produced by the action potential propagation is parallel to the sensing direction of the MTJs (Fig. 3(b)). More precisely, the sensors were positioned close to the CA3 region in order to sense the signals arising from the fibers linking the CA1 region to the CA3 region. Prior to magnetic detection, standard LFP recording were performed in order to verify the signals quality and to have reference values. Extracellular local field potentials were recorded using borosilicate glass electrodes (Kimble Chase, Vineland, NJ, USA) of 1-2 M $\Omega$  filled with artificial ACSF. Evoked post synaptic potential (EPSP) were evoked in granule cells layer in response to extracellular stimulation of the medial perforant path (PP) with a monopolar glass electrode (intensity: 150-300  $\mu\text{A}$ , duration: 1 ms; rectangular waveform) filled with ACSF and connected with an isolated pulse stimulator (A-M Systems, Carlsborg, WA). In Figure 3(c) the LFP extracellular recording signal, averaged over 10 acquisitions, is presented. The intense oscillation of the signal is due to artefacts, arising from current injected by the stimulating electrodes.<sup>26</sup> Note that the presence of the magnetic sensors underneath does not influence the LFP signal, which can be used to validate the magnetic platform. For the magnetic measurement, in order to minimize any interference arising from the stimulation signal, the chip and the power supplier were connected to a common ground. The output signal, averaged

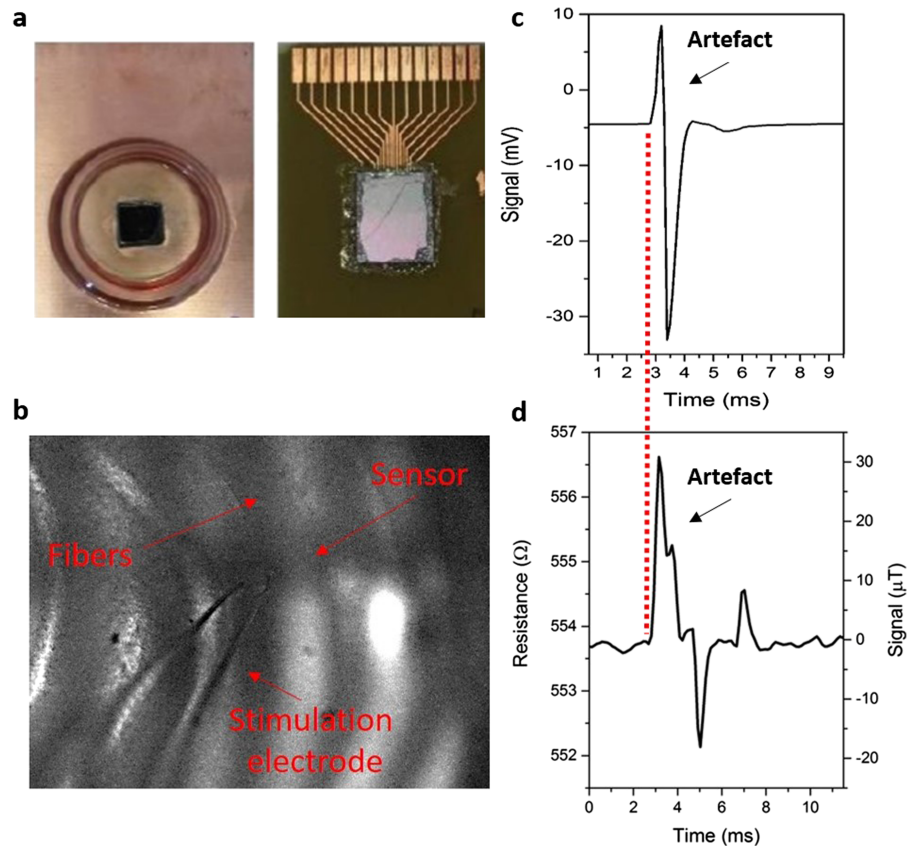


FIG. 3. (a) Top (left) and bottom (right) image of the chip attached to a custom PCB board with culture chamber. (b) Optical image of the brain slice on top of the chip. (c) Standard LFP measurement results showing the artefact and a small neural signal. (d) Result from the magnetic detection.

over 30 acquisitions, is presented in Fig.3 (d). The artefact signal is clearly visible with a signal to noise ratio (SNR) of 165, with the noise level calculated as the standard deviation of the signal over 800 values. In the averaged figure, as in most of the single acquisitions, the artefact is followed by a shorter signal, with a SNR of 120, after about 500  $\mu$ s. Such signal has a duration of 400  $\mu$ s and cannot be ascribed to the artefact. Due to the low statistics, however, it is currently not possible to confirm such signal to be the result of a magnetic detection and further work is needed.

## CONCLUSION

In this work, we presented a magnetic-based detection scheme for neural signal recording, via highly sensitive MTJs. We showed that such devices are promising tools for the detection of signals arising from brain slices when measurements are performed in a broadband configuration (1 Hz – 1 kHz). They also offer perspectives for the recording of single neuron activity, provided that the  $1/f$  noise of the MTJs is minimized or the magnetic field from neurons is modulated above the  $1/f$  corner. A suitable capping layer ensuring neuron viability over 2 weeks has been optimized and tested. Arrays of magnetic sensors have been integrated in a platform suitable for neural detection and the compatibility with standard LFP extracellular recording has been demonstrated. Finally, we presented some preliminary results concerning the magnetic detection of the brain slice activity with the developed platform and we showed its ability to successfully record the well known pre-peak artefact in the signal recorded immediately after stimulation. A further optimization of the sensitivity is on the way in order to detect the magnetic field pulse associated to the true neural signal.

**ACKNOWLEDGMENTS**

This work was funded by Fondazione Cariplo via the project UMANA (Project No. 2013-0735).

- <sup>1</sup> O. P. Hamill, A. Marty, E. Neher, B. Sakmann, and F. J. Sigworth, *Eur. J. Physiol.* **391**, 85 (1981).
- <sup>2</sup> G. Buzsaki, C. A. Anastassiou, and C. Koch, *Nat. Rev.* **13**, 407 (2012).
- <sup>3</sup> M. Pusch and E. Neher, *Eur. J. Physiol.* **490** (1990).
- <sup>4</sup> F. Heer, W. Franks, A. Blau, S. Taschini, C. Ziegler, A. Hierlemann, and H. Baltes, *Biosens. Bioelectron.* **20**, 358 (2004).
- <sup>5</sup> L. Berdondini, P. D. Van Der Wal, O. Guenat, N. F. De Rooij, M. Koudelka-Hep, P. Seitz, R. Kaufmann, P. Metzler, N. Blanc, and S. Rohr, *Biosens. Bioelectron.* **21**, 167 (2005).
- <sup>6</sup> S. Vassanelli and P. Fromherz, *J. Neurosci.* **19**, 6767 (1999).
- <sup>7</sup> F. Gullo, A. Maffezzoli, E. Dossi, M. Lecchi, and E. Wanke, *J. Neurosci. Methods* **203**, 407 (2012).
- <sup>8</sup> X. Duan, R. Gao, P. Xie, T. Cohen-Karni, Q. Qing, H. S. Choe, B. Tian, X. Jiang, and C. M. Lieber, *Nat. Nanotechnol.* **7**, 174 (2011).
- <sup>9</sup> J. T. Robinson, M. Jorgolli, A. K. Shalek, M.-H. H. Yoon, R. S. Gertner, and H. Park, *Nat. Nanotechnol.* **7**, 180 (2012).
- <sup>10</sup> C. Xie, Z. Lin, L. Hanson, Y. Cui, and B. Cui, *Nat. Nanotechnol.* **7**, 185 (2012).
- <sup>11</sup> V. Parpura, *Nat. Nano.* **7**, 143 (2012).
- <sup>12</sup> T. Chen, T. J. Wardill, Y. Sun, S. R. Pulver, S. L. Renninger, A. Baohan, E. R. Schreiter, R. A. Kerr, M. B. Orger, V. Jayaraman, L. L. Looger, K. Svoboda, and D. S. Kim, *Nature* **499** (2013).
- <sup>13</sup> L. Tian, S. A. Hires, T. Mao, D. Huber, M. E. Chiappe, S. H. Chalasani, L. Petreanu, J. Akerboom, S. A. McKinney, E. R. Schreiter, C. I. Bargmann, V. Jayaraman, K. Svoboda, and L. L. Looger, *Nat. Methods* **6** (2009).
- <sup>14</sup> J. F. Barry, M. J. Turner, J. M. Schloss, D. R. Glenn, Y. Song, M. D. Lukin, H. Park, and R. L. Walsworth, [arXiv:1602.01056](https://arxiv.org/abs/1602.01056) [Cond-Mat, Physics:physics, Physics:quant-Ph, Q-Bio] (2016).
- <sup>15</sup> A. Cooper, E. Magesan, H. N. Yum, and P. Cappellaro, *Nat Commun* **5**, 3141 (2014).
- <sup>16</sup> P. P. Freitas, R. Ferreira, S. Cardoso, and F. Cardoso, *J. Physics Condensed Matter* **19**, 165221 (2007).
- <sup>17</sup> P. P. Sharma, E. Albigsetti, M. Massetti, M. Scolari, M. Monticelli, M. Leone, F. Damin, G. Gervasoni, G. Ferrari, F. Salice, E. Cerquaglia, G. Falduti, M. Cretich, E. Marchisio, M. Chiari, M. Sampietro, D. Petti, and R. Bertacco, *Sensors Actuators B Chem.* (submitted) (2016).
- <sup>18</sup> M. Donolato, E. Sogne, B. T. Dalslet, M. Cantoni, D. Petti, J. Cao, F. Cardoso, S. Cardoso, P. P. Freitas, M. F. Hansen, and R. Bertacco, *Appl. Phys. Lett.* **98**, 73702 (2011).
- <sup>19</sup> J. Amaral, S. Cardoso, P. P. Freitas, and A. M. Sebastião, *J. Appl. Phys.* **109**, 07B308 (2011).
- <sup>20</sup> E. Albigsetti, D. Petti, M. Cantoni, F. Damin, A. Torti, M. Chiari, and R. Bertacco, *Biosens. Bioelectron.* **47**, 213 (2013).
- <sup>21</sup> E. Albigsetti, D. Petti, F. Damin, M. Cretich, A. Torti, M. Chiari, and R. Bertacco, *Sensors Actuators B Chem.* **200**, 39 (2014).
- <sup>22</sup> S. Yuasa and D. D. Djayaprawira, *J. Phys. D. Appl. Phys.* **40**, R337 (2007).
- <sup>23</sup> P. P. Sharma, E. Albigsetti, M. Monticelli, R. Bertacco, and D. Petti, *Sensors* **16** (2016).
- <sup>24</sup> P. Wiśniowski, J. M. Almeida, S. Cardoso, N. P. Barradas, and P. P. Freitas, *J. Appl. Phys.* **103**, 07A910 (2008).
- <sup>25</sup> D. Moretti, A. Garenne, E. Haro, F. P. de Gannes, I. Lagroye, P. Leveque, B. Veyret, and N. Lewis, *Bioelectromagnetics* **578** (2013).
- <sup>26</sup> E. Ferrea, A. Maccione, L. Medrihan, T. Nieuw, D. Ghezzi, P. Baldelli, F. Benfenati, and L. Berdondini, *Front. Neural Circuits* **6**, 1 (2012).
- <sup>27</sup> M. Sampietro, L. Fasoli, and G. Ferrari, *Rev. Sci. Instrum.* **70**, 2520 (1999).
- <sup>28</sup> P. Wisniowski, J. M. Almeida, and P. P. Freitas, *Current* **44**, 2551 (2008).
- <sup>29</sup> J. Amaral, V. Pinto, and T. Costa, *Magn. IEEE ...* **49**, 3512 (2013).
- <sup>30</sup> N. A. Stutzke, S. E. Russek, D. P. Pappas, and M. Tondra, *J. Appl. Phys.* **97**, 9 (2005).
- <sup>31</sup> J. Valadeiro, S. Cardoso, R. Macedo, A. Guedes, J. Gaspar, and P. Freitas, *Micromachines* **7**, 88 (2016).